Journal of Biomolecular NMR, **21:** 141–151, 2001.
KLUWER/ESCOM
© 2001 *Kluwer Academic Publishers. Printed in the Netherlands.*

Controlling residual dipolar couplings in high-resolution NMR of proteins by strain induced alignment in a gel

Yoshitaka Ishii[a], Michelle A. Markus[b,*] & Robert Tycko[a,**]
[a]*Laboratory of Chemical Physics, National Institute of Diabetes and Digestive and Kidney Diseases, National Institutes of Health, Bethesda, 20892-0520, U.S.A.;* [b]*Molecular Structural Biology Unit, National Institute of Dental and Craniofacial Research, National Institutes of Health, Bethesda, MA 20892-4307, U.S.A.*

Received 31 July 2001; Accepted 22 August 2001

Key words: dipolar couplings, polyacrylamide gel, protein NMR, structure determination, weak alignment

Abstract

Water-soluble biological macromolecules can be weakly aligned by dissolution in a strained, hydrated gel such as cross-linked polyacrylamide, an effect termed 'strain-induced alignment in a gel' (SAG). SAG induces nonzero nuclear magnetic dipole-dipole couplings that can be measured in high-resolution NMR spectra and used as structural constraints. The dependence of experimental ^{15}N-^{1}H dipolar couplings extracted from two-dimensional heteronuclear single quantum coherence (HSQC) spectra on several properties of compressed polyacrylamide, including the extent of compression, the polyacrylamide concentration, and the cross-link density, is reported for the B1 immunoglobulin binding domain of streptococcal protein G (protein G/B1, 57 residues). It is shown that the magnitude of macromolecular alignment can be widely varied by adjusting these properties, although the orientation and asymmetry of the alignment tensor are not affected significantly. The dependence of the ^{15}N relaxation times T_1 and T_2 of protein G/B1 on polyacrylamide concentration are also reported. In addition, the results of ^{15}N relaxation and HSQC experiments on the RNA binding domain of prokaryotic protein S4 from *Bacillus stearothermophilus* (S4 Δ41, residues 43–200) in a compressed polyacrylamide gel are presented. These results demonstrate the applicability of SAG to proteins of higher molecular weight and greater complexity. A modified in-phase/anti-phase (IPAP) HSQC technique is described that suppresses natural-abundance ^{15}N background signals from amide groups in polyacrylamide, resulting in cleaner HSQC spectra in SAG experiments. The mechanism of protein alignment in strained polyacrylamide gels is contrasted with that in liquid crystalline media.

Introduction

An important recent development in high-resolution biomolecular NMR has been the exploitation of structural information obtained from measurements of anisotropic interactions, such as nuclear magnetic dipole-dipole couplings, electric quadrupole couplings, and anisotropic chemical shifts, in spectra of weakly aligned biological macromolecules (Sanders et al., 1994; Sanders and Landis, 1995; Tolman et al., 1995; Tjandra et al., 1996, 1997; Tjandra and Bax, 1997; Clore et al., 1998; Hansen et al., 1998; Prosser et al., 1998; Cavagnero et al., 1999; Koenig et al., 1999; Ottiger and Bax, 1999; Sass et al., 1999; Barrientos et al., 2000; Sass et al., 2000; Tycko et al., 2000). Direct effects of residual anisotropic interactions on NMR spectra of dissolved molecules were observed earlier in experiments on small molecules aligned by magnetic fields (Lohman and MacLean, 1978; Bothnerby et al., 1981, 1985; Plantenga et al., 1981; Gayathri et al., 1982; Lisicki et al., 1988), electric fields (Plantenga and Maclean, 1980; Plantenga et al., 1980, 1982; Peshkovsky and McDermott, 1999; Riley and Augustine, 2000), and interactions with liquid crystalline solvents (Saupe and Englert, 1963; Emsley and Lindon, 1975). To create optimum weak align-

*Current address: Genetics Institute, Wyeth-Ayerst Research, 87 CambridgePark Drive, Cambridge, MA 02140, U.S.A.
**To whom correspondence should be addressed. E-mail: tycko@helix.nih.gov

ments of biomolecules, liquid crystalline mesophases aligned by an external magnetic field have been widely used (Tjandra and Bax, 1997; Tjandra et al., 1997; Clore et al., 1998; Hansen et al., 1998; Prosser et al., 1998; Cavagnero et al., 1999; Koenig et al., 1999; Ottiger and Bax, 1999; Sass et al., 1999; Barrientos et al., 2000). Although the tunable alignment obtained in liquid crystalline solvents has proven very powerful for extracting structural parameters for biomolecules, the degree of alignment induced by liquid crystalline solvents and the stability of liquid crystalline solutions are sensitive to experimental conditions such as temperature, ionic strength, and pH and may be dependent on properties of the biomolecular solute such as surface charge and hydrophobicity. Hence, attempts to align biomolecules in liquid crystalline solvents under experimental conditions of interest may not always be successful.

Very recently, we have demonstrated that weak alignment of proteins in high-resolution NMR can be achieved by an effect we call 'strain-induced alignment in a gel' (SAG) (Tycko et al., 2000). The same approach to biomolecular alignment has been independently demonstrated and investigated by Sass et al. (2000) In SAG experiments, a biological macromolecule is dissolved in a hydrated gel which is made anisotropic by mechanical strain (compressive strain in experiments reported to date, although extensive strain may also prove useful in future experiments). Interactions between the macromolecule and the gel then lead to anisotropy in the dynamic orientational distribution of the macromolecule, resulting in measurable dipolar couplings in the high-resolution NMR spectra. To date, SAG experiments have been performed with cross-linked polyacrylamide gels (Sass et al., 2000; Tycko et al., 2000), as commonly used in electrophoretic separations of proteins and nucleic acids, but similar results are expected from other hydrated gels. Our work on SAG was inspired by the earlier experiments of Deloche and Samulski (Deloche and Samulski, 1981) in which small organic molecules were weakly aligned by dissolution in strained rubbery polymers. We chose to examine polyacrylamide gels because they represent an elastically deformable medium analogous to a rubbery polymer but are compatible with hydrophilic solutes such as biomolecules.

Our previous report (Tycko et al., 2000) showed that SAG enables one to measure dipolar couplings over very wide ranges of temperature, pH, and ionic strength, due to the inherent stability of polyacrylamide gels with respect to these parameters. Here, we demonstrate that the degree of alignment obtained by SAG can be controlled by changing mechanical or chemical properties of the gel such as the extent of compression, the gel concentration, and the cross-link density for a given temperature and pH. Results of ^{15}N-^{1}H dipolar couplings are shown for the uniformly ^{15}N-labeled B1 immunoglobulin-binding domain of streptococcal protein G (protein G/B1), a small protein of known structure (Gronenborn et al., 1991; Gallagher et al., 1994), in uniaxially compressed polyacrylamide gels of varying composition and extent of compression. We also show that ^{15}N heteronuclear single-quantum coherence (HSQC) spectra of protein G/B1 and of the RNA binding domain of prokaryotic protein S4 from *Bacillus stearothermophilus* (S4 Δ41, residues 43–200) exhibit good resolution in SAG measurements, permitting the measurement of precise dipolar couplings. We describe a modification of the in-phase/anti-phase (IPAP) HSQC technique (Ottiger et al., 1998) that suppresses natural-abundance ^{15}N background signals in SAG experiments arising from the amide groups of polyacrylamide gels. Finally, we contrast the mechanism of protein alignment in strained polyacrylamide gels with that in liquid crystalline media.

Materials and methods

Uniformly ^{15}N-labeled protein G/B1 was prepared as described (Blanco et al., 1999). Our clone produced an N-formylated, 57-residue variant with an additional aspartate residue inserted between the first and second residues of the amino acid sequence used in earlier structural studies (Gronenborn et al., 1991; Gallagher et al., 1994). Comparison of ^{15}N HSQC spectra of the variant and the original sequence shows no significant differences, indicating no significant difference in their folded structures. Uniformly ^{15}N labeled S4 Δ41 was prepared as described by Markus et al. (1998) Polyacrylamide gels were prepared from aqueous solutions with acrylamide concentration C_A, ranging from 5.1% to 10.2% (w/v), and N,N′-methylenebisacrylamide cross-linker concentration C_B, ranging from 0.23% to 0.54% (w/v). Polymerization was initiated by addition of 0.08% (w/v) ammonium persulfate and 0.1% (v/v) N,N,N′-tetramethylethylenediamine immediately prior to casting. The values of C_A and C_B were varied to evaluate the effects of mechanical and chemical properties of the gel on measured dipolar couplings. As parameters

characterizing the composition of the gel, we use C_A and $F_{CL} = C_B/(C_A + C_B)$ to represent the concentration of the gel and cross-link density, respectively, where F_{CL} was varied from 2.9% to 5.0%. Gels were cast in the form of a rod with 3.4 mm diameter and approximately 8 cm length, using a cylindrical glass mold made from a medium-wall 5 mm NMR tube (524 PP, Wilmad Glass). The inner diameter of the mold is 0.8 mm less than that of the Shigemi microcell NMR sample tubes (BMS-005B, Shigemi Co., Ltd) used for NMR experiments (i.d. 4.2 mm). It was found that gels cast from the glass tube mold exhibit smoother surfaces than those cast from the teflon molds used for our initial SAG experiments (Tycko et al., 2000) and therefore induce less inhomogeneous broadening of the NMR signals. After polymerization was complete, the gels were washed with purified water and placed in a large excess volume of water with gentle agitation for more than three hours to permit unreacted acrylamide and initiators to diffuse out. Gels were then cut into initial lengths L_0 of approximately 19–22 mm.

For experiments on protein G/B1, the gel was gently wiped and soaked in 200 μl of 2.0 mM protein solution (pH 4.5) containing 20% D_2O in a Shigemi microcell NMR tube overnight. The pH was then adjusted to 4.6–4.7 with 1 M NaOH. The final protein concentration was approximately 1 mM, with 10% D_2O. For experiments on S4 Δ41, a gel with $L_0 =$ 22 mm was soaked in buffer solution (20 mM acetate, 250 mM KCl, 0.1 mM NaN_3, 0.1 mg/ml phenyl methyl sulfonyl fluoride, pH 5.5) for 2.5 h. The gel was then removed from the buffer and soaked in approximately 600 μl of protein solution overnight. The protein solution was 680 μM in ^{15}N-labeled S4 Δ41. Approximately 40 μl of buffer solution was added to the Shigemi microcell before the gel containing protein was added. The final concentration of S4 Δ41 was approximately 450 μM. For both proteins, the gel was compressed to a final length L with the Shigemi microcell plunger, with the extent of compression $R_L \equiv L/L_0$ ranging from 0.60 to 0.80. Use of a Shigemi microcell enables one to use a small volume of gel and readily adjust R_L while minimizing inhomogeneous broadening due to magnetic susceptibility mismatch. After compression, the plunger was held in place by wrapping with teflon tape and parafilm, taking care not to rotate the plunger and thereby tear the gel during the wrapping process. Experiments were performed at 25 °C and 37 °C for protein G/B1 and S4 Δ41, respectively.

It was found that water was gradually expelled from the gels under compression over a period of days, so that the volume of the gel, the effective extent of compression, and the observed dipolar couplings were slightly reduced. This gradual gel shrinkage did not affect the accuracy of the measured dipolar couplings in the present experiments, in which data acquisition times ranging from several hours to one day were used.

Experiments were performed with Bruker DMX spectrometers at ^{1}H NMR frequencies of 749.3 MHz for protein G/B1, and both 749.3 MHz and 499.5 MHz for S4 Δ41. No field dependence of dipolar couplings was detected. Average amide ^{15}N spin relaxation times T_1 and T_2 were measured using standard indirect detection methods (Kay et al., 1992). Two-dimensional ^{15}N/^{1}H HSQC spectra were recorded using the modified version of the IPAP-HSQC technique represented by the pulse sequence in Figure 1. Whereas the conventional IPAP-HSQC technique (Ottiger et al., 1998) contains two INEPT-type polarization transfer periods of length $(2J_{NH})^{-1}$ before the t_1 period, the second of which is present to generate the anti-phase doublet spectrum and absent to generate the in-phase doublet spectrum, the modified IPAP technique contains three such periods, the third of which is present to generate the in-phase doublet spectrum and absent to generate the anti-phase doublet spectrum. Ignoring pulse sequence imperfections and spin relaxation effects, the conventional and modified techniques lead to identical spectra for NH groups. However, the modified pulse sequence has the feature that the spin density operator for NH_2 groups is proportional to $2(I_{y1} + I_{y2})S_z$ at the beginning of t_1 when the third INEPT-type period is absent and to $(I_{x1} + I_{x2})$ when it is present, in the limit of negligible pulse sequence imperfections and with S and I representing ^{15}N and ^{1}H spin angular momenta, respectively. Then, since phase cycling in the pulse sequence selects for density operator components of the form $2I_zS_y$ or $2I_zS_x$ at the end of the t_1 period, signals from NH_2 groups are suppressed. In experiments with polyacrylamide gels, this removes strong, broad background signals that arise from natural-abundance ^{15}N. As in the conventional IPAP-HSQC technique (Ottiger et al., 1998), addition or subtraction of in-phase and anti-phase spectra yields a simplified HSQC spectrum containing only the upper or lower ^{15}N-^{1}H doublet components. Only in-phase doublet spectra are shown in Figures 3 and 6 below.

For measurements of ^{15}N-^{1}H doublet splittings for protein G/B1, HSQC spectra containing the upper and lower doublet components were processed separately.

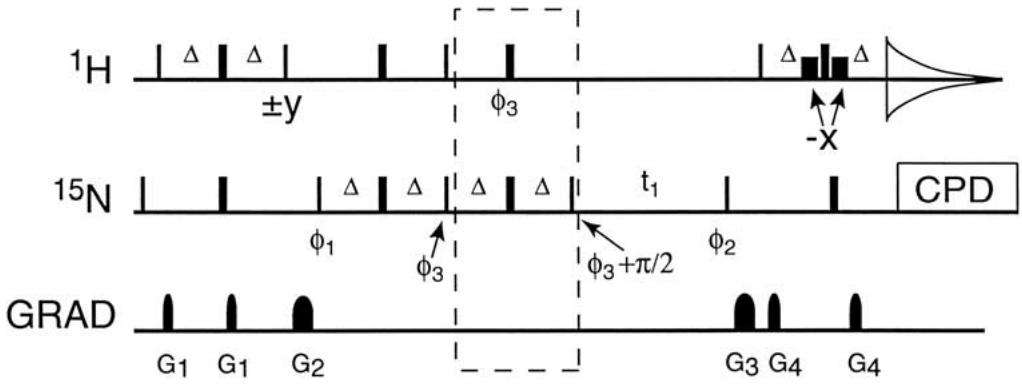

Figure 1. Modified in-phase/anti-phase heteronuclear single-quantum coherence (IPAP HSQC) technique designed to suppress natural-abundance ^{15}N signals from NH_2 groups of polyacrylamide gels. For the NH groups of a protein, an HSQC spectrum with in-phase doublets in the t_1 dimension is obtained when all pulses and delays are given. An HSQC spectrum with anti-phase doublets is obtained when pulses and delays in the dashed box are ommitted. CPD indicates composite-pulse decoupling. G_1, G_2, G_3, and G_4 are gradient pulses with different areas or directions. Δ delays are approximately 2.7 ms. Thin vertical bars represent π/2 pulses. Thick vertical bars represent π pulses. The last three ^1H pulses are for WATERGATE solvent suppression (Piotto et al., 1992). Radio-frequency phases are: ϕ_1 = x,x,−x,−x; ϕ_3 = x,−x,−x,x; ϕ_2 = x,x,x,x,−x,−x,−x,−x for in-phase spectrum and ϕ_2 = y,y,y,y,−y,−y,−y,−y for anti-phase spectrum. Phases indicated by ±y alternate on successive scans. Phases not labeled explicitly are x. During phase cycling, signals are coadded according to the sequence +,−,−,+,−,+,+,−. The imaginary part of the signal in the t_1 dimension is obtained by applying an additional π/2 phase shift to ϕ_2.

Maximum t_1 and t_2 values were 54.7 ms and 80.4 ms, respectively, and zero filling was applied in the t_1 dimension to produce a digital resolution of 0.85 Hz. A sine-bell function with initial phase 72° was applied for apodization in the t_1 dimension. A squared sine-bell function with initial phase 72° was applied in the t_2 dimension. Peak positions were determined using peak picking and peak fitting software in the nmrPipe program (Delaglio et al., 1995). Doublet splittings were determined by comparing peak tables for the upper and lower doublet components, with the condition that the two doublet components differ in their ^1H shifts by less than 2.0 Hz. For S4 Δ41, peak positions were determined with the PIPP program (Garrett et al., 1995) and the upper and lower doublet components were assigned by comparison with previously assigned HSQC spectra (Markus et al., 1998, 1999). Given that the residual dipolar couplings are smaller than the scalar couplings, ^{15}N-^1H dipolar couplings are defined as $D_{NH} - \Delta_{aq} - \Delta_{gel}$, where Δ_{aq} and Δ_{gel} are the absolute values of the doublet splittings in aqueous solution and in the strained gel. Alignment tensor principal values A, B, and C (units of Hz) and Euler angles α, β, γ that relate the alignment tensor principal axis system to a molecule-fixed axis system, defined by the atomic coordinates in Protein Data Bank file 1pga for protein G/B1, were determined by a least-squares fit of calculated dipolar couplings D_{fit} to the experimental couplings, with $D_{fit} = -(A \sin^2\theta \cos^2\phi + B \sin^2\theta \sin^2\phi + C \cos^2\theta)$, where and specify the direction of a given N-H internuclear vector in the alignment tensor principal axis system. (Note that the signs of both D_{NH} and D_{fit} in the expressions above are opposite to those in our earlier paper (Tycko et al., 2000), leading to the same signs for A, B, and C. As defined above, D_{NH} is $\gamma_N\gamma_H\hbar\langle(1 - 3\cos^2\xi)/R_{NH}^3\rangle/2\pi$, where γ_N and γ_H are the magnetogyric ratios of ^{15}N and ^1H, ξ is the angle between the internuclear vector and the magnetic field, R_{NH} is the internuclear distance, and the brackets represent an average over the molecular tumbling and internal motions.)

Results

Figure 2a shows the creation of optical birefringence in a polyacrylamide gel when uniaxial compressive strain is applied. Birefringence of the strained gel results from structural anisotropy that can produce weak dynamic alignment of molecules dissolved in the gel. Figures 2b and 2c show ^2H NMR spectra of D_2O in uniaxially compressed polyacrylamide gels under two different conditions. These spectra exhibit ^2H quadrupolar splittings due to weak alignment of D_2O molecules, in analogy to the results obtained for organic molecules in strained rubbery polymers by Deloche and Samulski (1981). The different splittings in Figures 2b and 2c indicate that the degree of alignment can be controlled by varying the gel con-

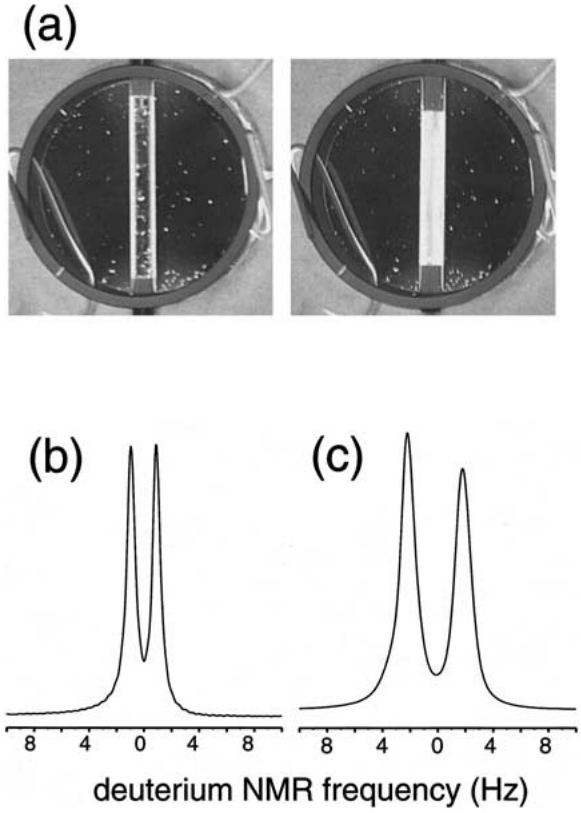

Figure 2. (a) Optical birefringence of a hydrated polyacrylamide gel induced by uniaxially compressive strain. The gel is contained in a standard 5 mm NMR tube, viewed between crossed polarizers with polarization axes at a 45° angle to the NMR tube, and illuminated from beneath. Gel concentration is $C_A = 11.5\%$ (w/v). Cross-link density is $F_{CL} = 5.2\%$ (w/w). The gel is compressed from initial length $L_0 = 35$ mm in the left panel to final length $L = 30$ mm in the right panel ($R_L - L/L_0 = 0.86$). Simultaneously, the gel diameter increases from 3.8 mm to 4.1 mm. (b) Deuterium NMR spectrum of D_2O (10% in H_2O) in a compressed polyacrylamide gel, contained in a Shigemi microcell tube and compressed with the microcell plunger, with $C_A = 7.7\%$ w/v, $F_{CL} = 2.9\%$ w/w, and $R_L = 0.77$. Spectrum is recorded at 115.0 MHz carrier frequency with single-pulse excitation and a single scan. The doublet splitting is due to a deuterium quadrupolar coupling induced by weak orientation of water molecules in the strained gel. (c) Same, but with $C_A = 7.7\%$ w/v, $F_{CL} = 5.1\%$ w/w, and $R_L = 0.70$.

ditions. No quadrupolar splittings are observed in ^2H NMR spectra of unstrained polyacrylamide gels. The relatively sharp linewidths in the quadrupolar doublets and the absence of significant unsplit ^2H NMR signal are indications of good uniformity of gel density and strain resulting from the protocols described above.

Figure 3a shows the amide region of a $^{15}N/^1H$ HSQC spectrum of uniformly ^{15}N-labeled protein G/B1 in a uniaxially compressed polyacrylamide gel ($C_A = 7.66\%$ w/v, $F_{CL} = 5.0\%$, and $R_L = 0.60$), obtained with the pulse sequence in Figure 1. Selected regions of HSQC spectra obtained in the strained gel and in aqueous solution are compared in Figures 3b and 3c. The doublet splittings differ in Figures 3b and 3c due to residual dipolar couplings induced by the SAG effect. Linewidths in the ^1H dimension are clearly greater in the strained gel. The increased linewidth is partially attributable to ^1H-^1H dipolar couplings and is similar to increased linewidths observed in liquid crystalline media. Slightly skewed crosspeak shapes in Figure 3b indicate a small degree of heterogeneity in the gel density and strain. The skew is larger for the upper doublet component because of cancellation between the effects of ^{15}N-^1H dipolar coupling and ^{15}N chemical shift anisotropy on the frequency of the lower doublet component. Chemical shifts of ^{15}N and ^1H nuclei in Figure 3b are slightly different from those in Figure 3c. These differences in shifts are due in part to chemical shift anisotropy induced by SAG and in part to a small pH difference between the two samples. Overall, the data in Figure 3 demonstrate that high-resolution spectra and precise dipolar couplings can be obtained with SAG in the case of small proteins. Results for the larger protein S4 Δ41 are discussed below.

Dipolar couplings D_{NH} for protein G/B1 were measured from $^{15}N/^1H$ HSQC spectra in polyacrylamide gels with various compositions and extents of compression. Alignment tensor principal values and principal axis directions were determined in each case. The results are summarized in Figure 4 and Table 1. Figure 4a shows the correlation of dipolar couplings obtained from HSQC spectra of protein G/B1 in gels with a fixed concentration and cross-link density ($C_A = 7.7\%$ w/v, $F_{CL} = 5.0\%$ w/w), but with different extents of compression ($R_L = 0.70$ and $R_L = 0.60$). A linear fit to the data in Figure 4a yields a slope of 1.33, with greater couplings at the smaller value of R_L, suggesting that the degree of alignment may be roughly proportional to $(1 - R_L)$. The small degree of scatter in Figure 4a suggests that the orientation and asymmetry $\eta \equiv (B - A)/C$ of the alignment tensor do not change as the magnitude of alignment increases, as verified quantitatively in Table 1. Figures 4b and 4c show correlations of dipolar couplings in gels with fixed cross-link density and compression ($F_{CL} = 5.0\%$ w/w, $R_L = 0.70$), but with different polyacrylamide concentrations ($C_A = 5.1\%$, 7.7%, and 10.2% w/v). The magnitude of alignment increases with gel concentration in a strongly nonlinear manner. The orientation and asymmetry of

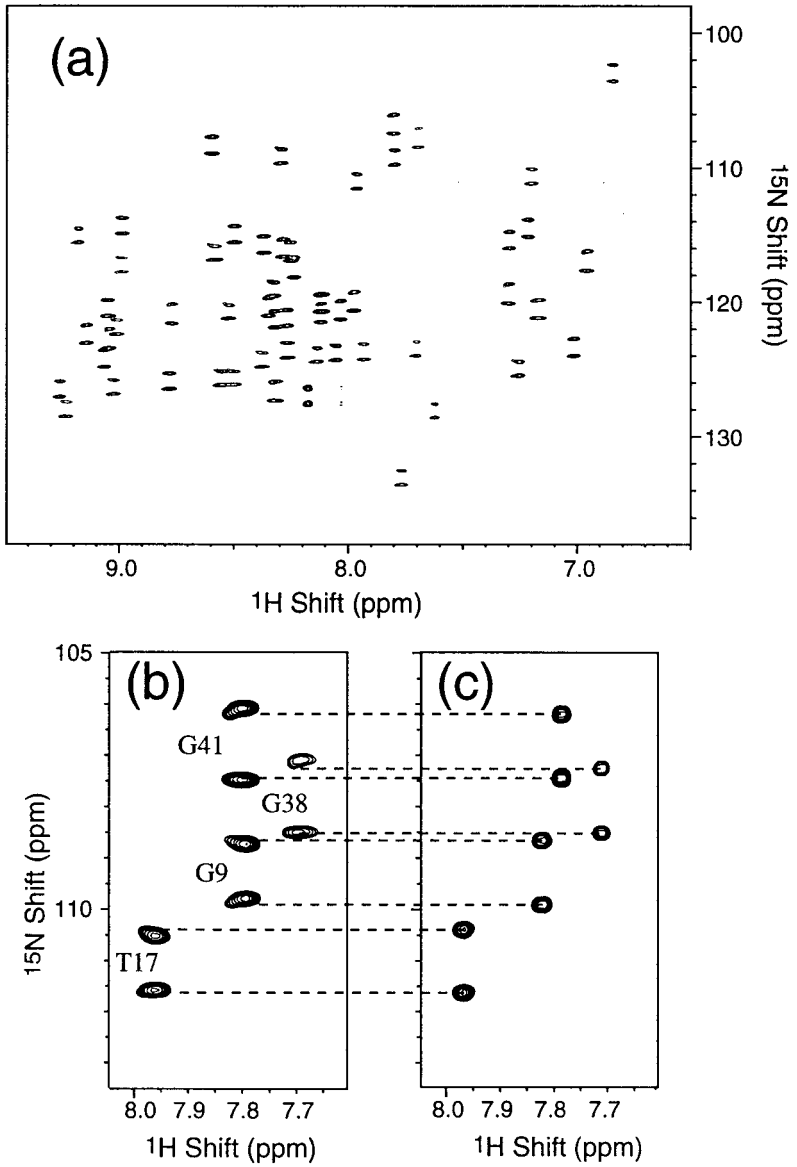

Figure 3. (a) Amide region of the $^{15}N/^{1}H$ HSQC spectrum of uniformly ^{15}N-labeled protein G/B1 at pH 4.6 and 25 °C in a compressed polyacrylamide gel with $C_A = 7.7\%$ w/v, $F_{CL} = 5.0\%$ w/w, and $R_L = 0.60$. Data were collected at an ^{1}H NMR frequency of 749.3 MHz using the pulse sequence in Figure 1 (in-phase spectrum only). Maximum t_1 and t_2 values are 54.7 ms and 80.4 ms, respectively. Sine-bell functions with initial phases of 72° and 82.8° were applied for apodization in the t_1 and t_2 dimensions, respectively. (b) Expanded region of the HSQC spectrum in the compressed gel. (c) Expanded region of an HSQC spectrum in aqueous solution. Dashed lines permit comparisons of doublet splittings. Splittings are found both to increase (residues G41 and G38) and to decrease (residues G9 and T17), reflecting the creation of residual ^{15}N-^{1}H dipolar couplings in the strained gel.

the alignment tensor are unaffected to within experimental error. Figures 4d and 4e show correlations of dipolar couplings in gels with fixed concentration and compression ($C_A = 7.7\%$ w/v, $R_L = 0.70$), but with different cross-link densities ($F_{CL} = 2.9\%$, 4.0%, and 5.0% w/w). Again, a strongly nonlinear increase in alignment with increasing cross-link density is observed, but the asymmetry and orientation of the alignment tensor do not change to within experimental error.

Figure 5 shows the dependence of the ^{15}N spin relaxation times T_1 and T_2 on C_A for protein G/B1,

Table 1. Dependence of the best-fit alignment tensor for protein G/B1 in a uniaxially compressed polyacrylamide gel on the polyacrylamide concentration, the cross-link density, and the extent of compression

C_A[a]	F_{CL}[b]	R_L[c]	A, B, C (Hz)[d]	α,β,γ (deg)[e]	η[f]	N[g]
7.7%	5.0%	0.70	−15.2± 0.9, −1.3±0.7, 16.5±0.7	167 ± 2, 112 ±2, 135 ±4	0.84±0.08	45
7.7%	5.0%	0.60	−19.7± 1.1, −2.0±0.9, 21.7±0.8	170 ± 3, 114 ±2, 139 ±3	0.82±0.08	44
5.1%	5.0%	0.70	−3.1± 0.4, −0.6±0.3, 3.7±0.4	172 ± 6, 115 ±4, 141 ±9	0.67±0.16	45
10.2%	5.0%	0.70	−24.8± 2.3, −3.0±1.5, 27.8±2.0	169 ± 3, 114 ±3, 136 ±5	0.79±0.10	16
7.7%	2.9%	0.70	−8.9±−2.1, 1.5±1.5, 7.4±1.1	174.0±14, 118.0±9, 131.0±9	1.4 ±0.4	37
7.7%	4.0%	0.70	−10.6± 1.2, −0.4±0.8, 11.0±0.9	170 ± 5, 112 ±4, 135 ±6	0.93±0.15	42

[a]Acrylamide concentration (w/v).
[b]Cross-link density (w/w).
[c]Extent of compression (L/L_0).
[d]Principal values of the best-fit alignment tensor, with $A < B < C$. Error limits correspond to variations in individual parameters that produce a change in χ^2 of one unit after reoptimization of other parameters to minimize χ^2.
[e]Euler angles describing the orientation of the best-fit alignment tensor relative to the crystal structure (PDB file 1pga). Note that all calculated dipolar couplings are invariant to the symmetry operations $(\alpha,\beta,\gamma) \leftrightarrow (\alpha,\beta,\gamma+\pi)$, $(\alpha,\beta,\gamma) \leftrightarrow (\alpha+\pi,\pi-\beta,\pi-\gamma)$, and $(\alpha,\beta,\gamma) \leftrightarrow (\alpha+\pi,\pi-\beta,-\gamma)$, which correspond to rotations of the alignment tensor principal axis system by π about the C, B, or A principal axes.
[f]Asymmetry of alignment tensor, with $\eta \equiv (B - A)/C$.
[g]Number of dipolar couplings analyzed.

at $R_C = 0.70$ and $F_{CL} = 5.0\%$ w/w. A small increase in T_1 in the gel, relative to aqueous solution, and a monotonic decrease in T_2 with increasing C_A are observed. Similar results for ^{15}N-labeled ubiquitin in polyacrylamide gels have been reported by Sass et al. (2000) The data on protein G/B1 and ubiquitin, as well as the results for S4 Δ41 shown below and for HIV-1 $Nef^{\Delta 2-39}$ reported by Sass et al. (2000), indicate that a useful degree of alignment of proteins ranging in molecular weight from 6 kD to at least 20 kD can be obtained in SAG experiments without prohibitive reductions in T_2. In the case of protein G/B1, a polyacrylamide gel with $C_A = 7.7\%$ w/v, $F_{CL} = 5.0\%$ w/w, and $R_L = 0.70$ produces D_{NH} values ranging from −14.8 to 17.2 Hz with a reduction of T_2 by a factor of 1.25.

Figure 6 shows the HSQC spectrum of uniformly ^{15}N-labeled S4 Δ41 obtained at 749.3 MHz in a compressed polyacrylamide gel with $C_A = 5.1\%$ w/v, $F_{CL} = 5.0\%$ w/w, and $R_L = 0.70$. Good spectral resolution is obtained under these conditions, and experimental D_{NH} values range from −9.5 to 5.6 Hz. The expanded region in Figure 6b corresponds to that previously published by Markus et al. (1999) (see Figure 4 of this reference) for the same protein in a liquid crystalline bacteriophage Pf1 solution with approximately the same pH and salt concentration. Although D_{NH} values in the Pf1 solution were larger (−28 Hz to 26 Hz), the spectral resolution in the polyacrylamide gel is significantly higher, indicating that dipolar couplings can be measured with similar precision for this protein. It is noteworthy that the range of D_{NH} values for S4 Δ41 is larger by a factor of two than those for protein G/B1 with the same gel conditions.

In earlier measurements on S4 Δ41 in a DMPC/DHPC bicelle medium, stability of the liquid crystalline phase was apparently impaired by the protein, and successful measurements were limited to a protein concentration of 100 μM (Markus et al., 1999). No protein aggregation or sample instability was observed in the present SAG experiments at 450 μM protein concentration. In the 5.1% w/v gel, the average ^{15}N T_2 for S4 Δ41 was 79 ± 9 ms, compared with a value of 86 ± 8 ms in aqueous solution. D_{NH} values determined from SAG experiments were used in X-PLOR calculations, together with NOE and dihedral angle restraints. The resulting structure of S4 Δ41 was essentially the same as the structure previously determined using D_{NH}values measured in a Pf1 solution.

Discussion

In a previous report (Tycko et al., 2000), we introduced the SAG technique and demonstrated that this technique is effective over wide ranges of temperature (at least 5 °C to 45 °C), pH (at least 2.0 to 8.5) and ionic strength (NaCl concentrations from 0 mM to at least 200 mM). These initial demonstrations were carried out on uniformly ^{15}N-labeled protein G/B1.

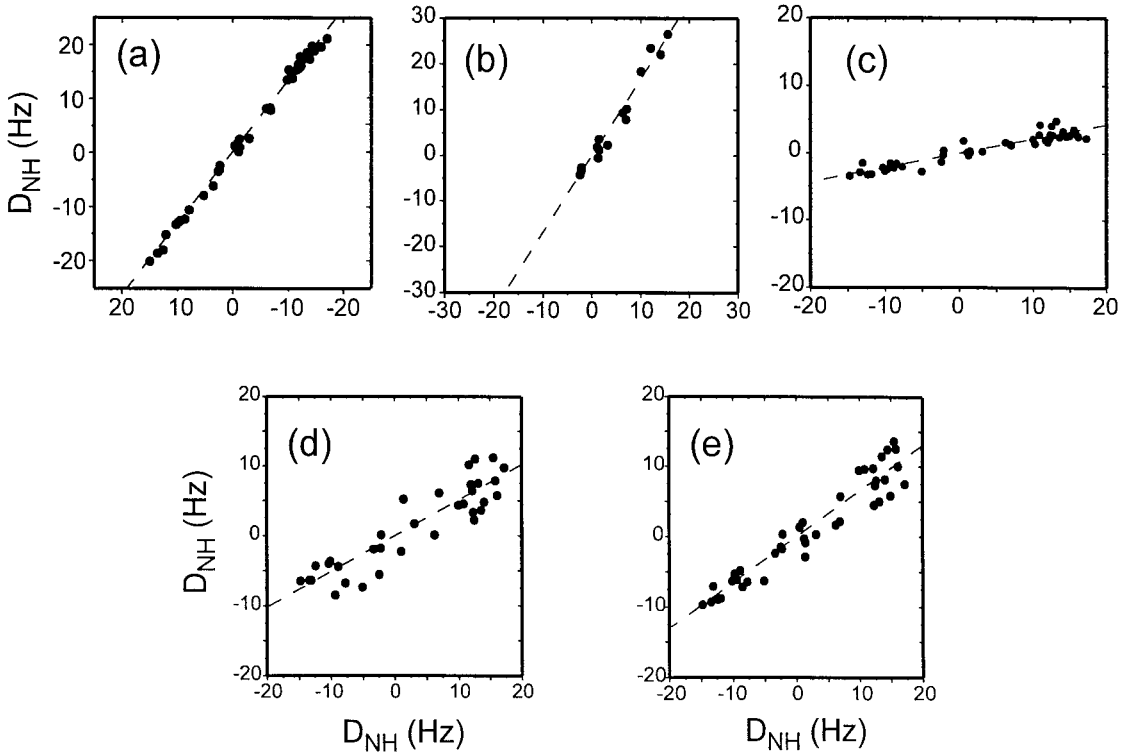

Figure 4. Dependence of experimental ^{15}N-^{1}H dipolar couplings on gel conditions. All data are for uniformly ^{15}N-labeled protein G/B1 at pH 4.6 and 25 °C in uniaxially compressed polyacrylamide gels. Each data point correlates the observed couplings for a single NH group under two conditions. Dashed lines are linear least-squares fits with the intercept constrained to be zero. (a) Dependence on extent of gel compression, for $C_A = 7.7\%$ w/v and $F_{CL} = 5.0\%$ w/w. Vertical axis is dipolar splitting observed with $R_L = 0.60$. Horizontal axis is dipolar splitting observed with $R_L = 0.70$. Slope of least-squares fit is $S_{LLS} = 1.33 \pm 0.01$, with correlation coefficient $R = 0.997$. (b) Dependence on polyacrylamide concentration, with $F_{CL} = 5.0\%$ w/w and $R_L = 0.70$. Vertical axis is $C_A = 5.1\%$ w/v. Horizontal axis is 7.7% w/v. $S_{LLS} = 0.21 \pm 0.12$, $R = 0.942$. (c) Dependence on polyacrylamide concentration, with $F_{CL} = 5.0\%$ w/w and $R_L = 0.70$. Vertical axis is $C_A = 10.2\%$ w/v. Horizontal axis is 7.7% w/v. $S_{LLS} = 1.68 \pm 0.07$, $R = 0.984$. (d) Dependence on cross-link density, with $C_A = 7.7\%$ w/v and $R_L = 0.70$. Vertical axis is $F_{CL} = 2.9\%$ w/w. Horizontal axis is $F_{CL} = 5.0\%$ w/w. $S_{LLS} = 0.51 \pm 0.04$, $R = 0.905$. (e) Dependence on cross-link density, with $C_A = 7.7\%$ w/v and $R_L = 0.70$. Vertical axis is $F_{CL} = 4.0\%$ w/w. Horizontal axis is $F_{CL} = 5.0\%$ w/w. $S_{LLS} = 0.65 \pm 0.03$, $R = 0.957$.

Independently, Sass et al. demonstrated weak alignment and measurements of residual ^{15}N-^{1}H dipolar couplings in strained polyacrylamide gels for two proteins (Sass et al., 2000), namely ubiquitin and HIV-1 Nef$^{\Delta 2-39}$. In the experiments described above, we have taken additional data on protein G/B1 and on S4 Δ41. Taken together, these results suggest the general applicability of the SAG technique for weak alignment of proteins with molecular weights up to at least 20 kD.

The results presented above for protein G/B1 show that the magnitude of alignment for a given protein may be controlled by varying the polyacrylamide concentration, the extent of compression, and the cross-link density. The optimal conditions are likely to depend on the molecular weight, shape, and possibly other properties of the protein, and may involve a trade-off between the magnitude of alignment and the reduction in T_2 relaxation times. For HIV-1 Nef$^{\Delta 2-39}$, Sass et al. report D_{NH} values ranging from approximately -20 Hz to $+10$ Hz and an average ^{15}N T_2 value of 45 ms in a gel with $C_A = 7\%$ w/v, $F_{CL} = 2.6\%$ w/w, and $R_L = 0.75$ (Sass et al., 2000). For ubiquitin, Sass et al. report D_{NH} values ranging from approximately -5 Hz to $+5$ Hz and an average ^{15}N T_2 value of 110 ms under similar conditions, but with $R_L = 0.80$ (Sass et al., 2000). In gels with $C_A = 5.1\%$ w/v, $F_{CL} = 5.0\%$ w/w, and $R_L = 0.70$, we observe D_{NH} values ranging from -9.5 Hz to $+5.6$ Hz for S4 Δ41 and D_{NH} values ranging from approximately -3 Hz to $+4$ Hz from protein G/B1.

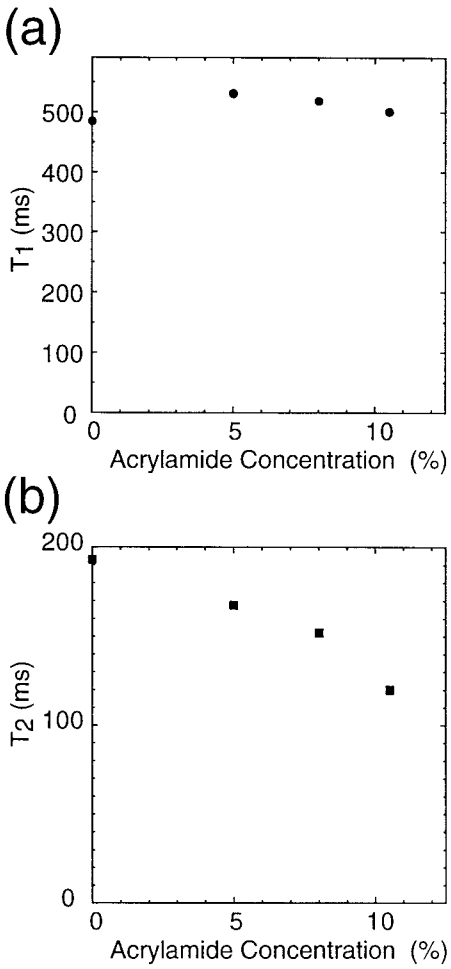

Figure 5. Dependence of ^{15}N spin relaxation times T_1 and T_2 for uniformly ^{15}N-labeled protein G/B1 on polyacrylamide concentration (C_A). Relaxation times are average values for all protein amide groups, determined by indirect-detection methods at a 749.3 MHz ^{1}H NMR frequency, pH = 4.6 and 25 °C. Data at $C_A > 0$ were obtained in gels with $F_{CL} = 5.0\%$ w/w and $R_L = 0.70$. Data at $C_A = 0$ were obtained in aqueous solution.

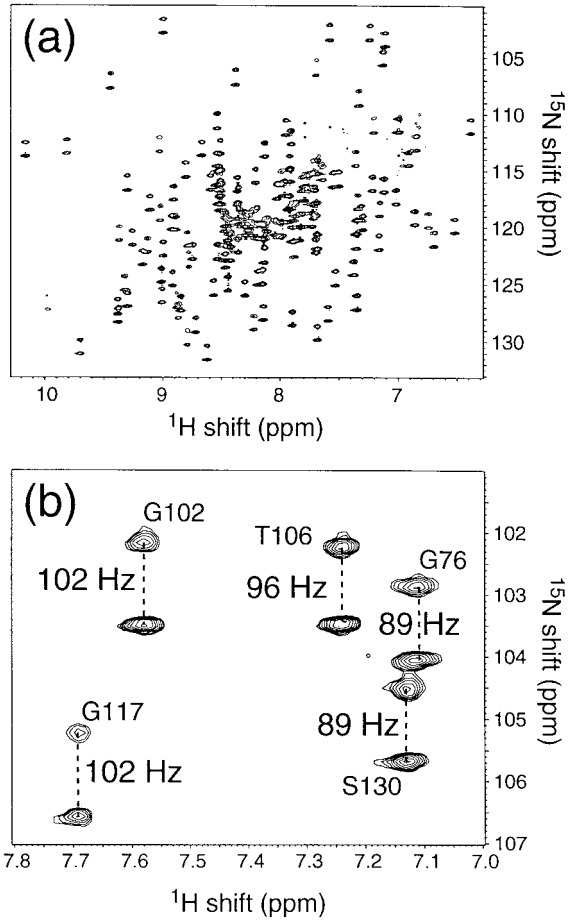

Figure 6. (a) ^{1}H/^{15}N HSQC spectrum of uniformly ^{15}N-labeled S4 Δ41 in a uniaxially compressed polyacrylamide gel. Data were collected at 749.3 MHz and 37 °C on approximately 450 μM of S4 Δ41 in buffer solution (20 mM acetate, 250 mM KCl, 0.1 mM Na azide, 0.1 mg/ml PMSF, pH 5.5). Gel conditions were $C_A = 5.1\%$ w/v, $F_{CL} = 5.0\%$ w/w, and $R_L = 0.70$. Maximum t_1 and t_2 values are 54.7 ms and 80.4 ms, respectively. Linear prediction was applied in the t_1 dimension. A sine-bell function with initial phase 82.8° was applied for apodization in t_1, while a squared sine-bell function with initial phase 72° was applied in t_2. (b) Expanded region of the HSQC spectrum, showing the variations in doublet splittings due to dipolar couplings arising from weak alignment of S4 Δ41 in the strained gel.

Effective pore radii (r_p) for polyacrylamide gels have been reported by Stellwagen (Stellwagen, 1997). These values of r_p are determined from experimental measurements of the dependence of the electrophoretic mobility of linear DNA fragments on the radius of gyration of the DNA. At $F_{CL} = 5\%$ w/w, r_p is approximately 30 nm, 22 nm and 19 nm for gels with C_A of 5.11, 7.66, and 10.21% w/v, respectively. At $F_{CL} = 3\%$, r_p values are approximately four times larger. For comparison, the dimensions of protein G/B1 are roughly 2.8 nm × 1.5 nm × 1.3 nm (Gronenborn et al., 1991; Gallagher et al., 1994). The dimensions of S4 Δ41 are roughly 6 nm × 4 nm × 4 nm (Markus et al., 1998, 1999). Thus, under the conditions of successful SAG experiments, the effective pore radius greatly exceeds the protein dimensions. In this respect, SAG experiments appear similar to alignment experiments using bicelles, in which the average spacing between bicelles also greatly exceeds the dimensions of the biomolecular solute. However, the precise structural meaning of r_p and its relevance to SAG experiments are unclear. In fact, the mech-

anism of protein alignment in a strained gel appears qualitatively different from that in a liquid crystalline bicelle medium. As shown by Zweckstetter and Bax (2000), alignment in a bicelle medium can be understood through a simple model in which the bicelles act as rigid walls, widely separated by solvent, that obstruct rotational diffusion of the solute only during collisions with the walls. Solute molecules tumble freely most of the time. In contrast, a polyacrylamide gel is a hydrated mesh of single polymer chains with random entanglements and cross-links. At $C_A - 8\%$ w/v, the average separation between polymer chains is roughly 2 nm. A protein in a polyacrylamide gel may then be viewed as being in constant contact with the flexible polyacrylamide chains, which exert a continuous, time-dependent aligning field on the protein as it diffuses translationally. In an anisotropic gel, the time average of the aligning field sampled by the diffusing protein (over the millisecond time scales relevant to the measurement of residual dipolar couplings) is nonzero and relatively uniform (provided the gel composition and strain are uniform). Two manifestations of the qualitative differences between alignment in a bicelle medium and alignment in a strained gel are (1) the fact that T_2 relaxation times are significantly affected by the gel concentration (see Figure 5), whereas T_2 relaxation times in a bicelle medium are not significantly different than in aqueous solution (Bax and Tjandra, 1997), and (2) the fact that the magnitude of alignment in a polyacrylamide gel is a strongly nonlinear function of gel concentration (see Table 1), whereas the magnitude of alignment in a bicelle medium is proportional to the bicelle concentration (Bax and Tjandra, 1997). Similar dependences of T_2 and the magnitude of alignment on gel concentration have been reported for ubiquitin by Sass et al. (2000).

A detailed understanding of the interactions between a biological macromolecule and the gel that determine the experimentally observed alignment tensor has not yet been achieved, but several facts are worth noting: (1) Because the polyacrylamide gel is uncharged, electrostatic interactions probably play a minor role. Use of a modified gel with charged groups might alter this situation; (2) we have previously reported that the principal axes of the alignment tensor for protein G/B1 in a compressed polyacrylamide gel are nearly coincident with the principal axes of the moment of inertia tensor (Tycko et al., 2000). The principal axes of the alignment tensor for protein G/B1 in a compressed polyacrylamide gel are also nearly coincident with those in a bicelle medium (Clore et al., 1998), but the reported asymmetry parameter $\eta = 0.35$ in the bicelle medium is significantly smaller than in the gel. Alignment of protein G/B1 in a liquid crystalline Pf1 solution leads to quite different directions of the alignment tensor principal axes, and to $\eta \approx 1.0$ (Clore et al., 1998); (3) In both the compressed polyacrylamide gel and the liquid crystalline DMPC/DHPC bicelle solution, the alignment tensor principal axis for S4 $\Delta 41$ that corresponds to the principal value with the greatest magnitude (A axis in the SAG measurements) is nearly coincident with the long axis of this rod-like protein (Markus et al., 1999). The signs of the alignment tensor principal values are reversed in the two media, indicating preferential alignment of the long axis of the protein parallel to the magnetic field in the bicelle solution and perpendicular to the magnetic field in the compressed gel. Alignment tensor asymmetry parameters are $\eta = 0.33$ in the gel with $C_A = 5.1\%$ and $\eta = 0.54$ in the bicelle solution. In contrast, the asymmetry parameter is $\eta = 0.97$ in Pf1 solution, where electrostatic interactions are expected to affect the alignment strongly; (4) Sass et al. have reported that the alignment tensor principal axis directions and asymmetry for ubiquitin in a compressed polyacrylamide gel are independent of gel concentration (Sass et al., 2000), as shown above for protein G/B1. They also report that the alignment tensor axes for ubiquitin in a compressed gel are nearly coincident with those in a bicelle medium, but that the asymmetry parameter is significantly larger in the gel, as in the case of protein G/B1.

Acknowledgements

This work was supported in part by the Intramural AIDS Targeted Antiviral Program of the Office of the Director of the National Institutes of Health. YI received fellowship support from the Japan Society for the Promotion of Science. We thank Dr Francisco J. Blanco for providing ^{15}N-labeled protein G/B1 samples used in this work. We thank Dr Dennis A. Torchia for suggesting the modified IPAP HSQC pulse sequence described in this paper and for a constructively critical reading of the manuscript.

References

Barrientos, L.G., Dolan, C. and Gronenborn, A.M. (2000) *J. Biomol. NMR*, **16**, 329–337.

Bax, A. and Tjandra, N. (1997) *J. Biomol. NMR*, **10**, 289–292.

Blanco, F.J., Angrand, I. and Serrano, L. (1999) *J. Mol. Biol.*, **285**, 741–753.

Bothnerby, A.A., Domaille, P.J. and Gayathri, C. (1981) *J. Am. Chem. Soc.*, **103**, 5602–5603.

Bothnerby, A.A., Gayathri, C., Vanzijl, P.C.M., Maclean, C., Lai, J.J. and Smith, K.M. (1985) *Magn. Reson. Chem.*, **23**, 935–938.

Cavagnero, S., Dyson, H.J. and Wright, P.E. (1999) *J. Biomol. NMR*, **13**, 387–391.

Clore, G.M., Starich, M.R. and Gronenborn, A.M. (1998) *J. Am. Chem. Soc.*, **120**, 10571–10572.

Delaglio, F., Grzesiek, S., Vuister, G.W., Zhu, G., Pfeifer, J. and Bax, A. (1995) *J. Biomol. NMR*, **6**, 277–293.

Deloche, B. and Samulski, E.T. (1981) *Macromolecules*, **14**, 575–581.

Emsley, J.W. and Lindon, J.C. (1975) *'NMR Spectroscopy Using Liquid Crystal Solvents'*, Pergamon Press, New York, NY.

Gallagher, T., Alexander, P., Bryan, P. and Gilliland, G.L. (1994) *Biochemistry*, **33**, 4721–4729.

Garrett, D.S., Gronenborn, A.M. and Clore, G.M. (1995) *J. Cell. Biochem. Suppl.*, **21B**, 71–71.

Gayathri, C., Bothnerby, A.A., Vanzijl, P.C.M. and Maclean, C. (1982) *Chem. Phys. Lett.*, **87**, 192–196.

Gronenborn, A.M., Filpula, D.R., Essig, N.Z., Achari, A., Whitlow, M., Wingfield, P.T. and Clore, G.M. (1991) *Science*, **253**, 657–661.

Hansen, M.R., Mueller, L. and Pardi, A. (1998) *Nat. Struct. Biol.*, **5**, 1065–1074.

Kay, L.E., Nicholson, L.K., Delaglio, F., Bax, A. and Torchia, D.A. (1992) *J. Magn. Reson.*, **97**, 359–375.

Koenig, B.W., Hu, J.S., Ottiger, M., Bose, S., Hendler, R.W. and Bax, A. (1999) *J. Am. Chem. Soc.*, **121**, 1385–1386.

Lisicki, M.A., Mishra, P.K., Bothnerby, A.A. and Lindsey, J.S. (1988) *J. Phys. Chem.*, **92**, 3400–3403.

Lohman, J.A.B. and MacLean, C. (1978) *Chem. Phys.*, **35**, 269–274.

Markus, M.A., Gerstner, R.B., Draper, D.E. and Torchia, D.A. (1999) *J. Mol. Biol.*, **292**, 375–387.

Markus, M.A., Gerstner, R.B., Draper, R.B. and Torchia, D.A. (1998) *EMBO J.*, **17**, 4559–4571.

Ottiger, M. and Bax, A. (1999) *J. Biomol. NMR*, **13**, 187–191.

Ottiger, M., Delaglio, F. and Bax, A. (1998) *J. Magn. Reson.*, **131**, 373–378.

Peshkovsky, A. and McDermott, A.E. (1999) *J. Phys. Chem.*, **A103**, 8604–8611.

Piotto, M., Saudek, V. and Sklenar, V. (1992) *J. Biomol. NMR*, **2**, 661–665.

Plantenga, T.M. and Maclean, C. (1980) *Chem. Phys. Lett.*, **75**, 294–297.

Plantenga, T.M., Bulsink, H., Maclean, C. and Lohman, J.A.B. (1981) *Chem. Phys.*, **61**, 271–280.

Plantenga, T.M., Dekanter, F.J.J., Bulsink, H. and Maclean, C. (1982) *Chem. Phys.*, **65**, 77–81.

Plantenga, T.M., Ruessink, B.H. and Maclean, C. (1980) *Chem. Phys.*, **48**, 359–368.

Prosser, R.S., Losonczi, J.A. and Shiyanovskaya, I.V. (1998) *J. Am. Chem. Soc.*, **120**, 11010–11011.

Riley, S.A. and Augustine, M.P. (2000) *J. Phys. Chem.*, **A104**, 3326–3331.

Sanders, C.R. and Landis, G.C. (1995) *Biochemistry*, **34**, 4030–4040.

Sanders, C.R., Hare, B.J., Howard, K.P. and Prestegard, J.H. (1994) *Prog. Nucl. Magn. Reson. Spectr.*, **26**, 421–444.

Sass, J., Cordier, F., Hoffmann, A., Cousin, A., Omichinski, J.G., Lowen, H. and Grzesiek, S. (1999) *J. Am. Chem. Soc.*, **121**, 2047–2055.

Sass, H.J., Musco, G., Stahl, S.J., Wingfield, P.T. and Grzesiek, S. (2000) *J. Biomol. NMR*, **18**, 303–309.

Saupe, A. and Englert, G. (1963) *Phys. Rev. Lett.*, **11**, 462.

Stellwagen, N.C. (1997) *Electrophoresis*, **18**, 34–44.

Tjandra, N. and Bax, A. (1997) *Science*, **278**, 1697–1697.

Tjandra, N., Grzesiek, S. and Bax, A. (1996) *J. Am. Chem. Soc.*, **118**, 6264–6272.

Tjandra, N., Omichinski, J.G., Gronenborn, A.M., Clore, G.M. and Bax, A. (1997) *Nat. Struct. Biol.*, **4**, 732–738.

Tolman, J.R., Flanagan, J.M., Kennedy, M.A. and Prestegard, J.H. (1995) *Proc. Natl. Acad. Sci. USA*, **92**, 9279–9283.

Tycko, R., Blanco, F.J. and Ishii, Y. (2000) *J. Am. Chem. Soc.*, **122**, 9340–9341.

Zweckstetter, M. and Bax, A. (2000) *J. Am. Chem. Soc.*, **122**, 3791–3792.